
Principled Federated Random Forests for Heterogeneous Data

Rémi Khellaf¹ Erwan Scornet² Aurélien Bellet¹ Julie Josse¹

Abstract

Random Forests (RF) are among the most powerful and widely used predictive models for centralized tabular data, yet few methods exist to adapt them to the federated learning setting. Unlike most federated learning approaches, the piecewise-constant nature of RF prevents exact gradient-based optimization. As a result, existing federated RF implementations rely on unprincipled heuristics: for instance, aggregating decision trees trained independently on clients fails to optimize the global impurity criterion, even under simple distribution shifts. We propose FedForest, a new federated RF algorithm for horizontally partitioned data that naturally accommodates diverse forms of client data heterogeneity, from covariate shift to more complex outcome shift mechanisms. We prove that our splitting procedure, based on aggregating carefully chosen client statistics, closely approximates the split selected by a centralized algorithm. Moreover, FedForest allows splits on client indicators, enabling a non-parametric form of personalization that is absent from prior federated random forest methods. Empirically, we demonstrate that the resulting federated forests closely match centralized performance across heterogeneous benchmarks while remaining communication-efficient.

1. Introduction

Random Forests (RFs) (Breiman, 2001) are ensembles of CART decision trees (Breiman et al., 1984) that recursively partition the feature space into regions, referred to as nodes, by selecting splits that maximize an impurity reduction criterion (e.g., variance or Gini). Predictions are then produced by aggregating the outcomes associated with the terminal nodes, commonly called leaves. Despite the deep learning

revolution, RFs remain among the state-of-the-art and most widely used predictors for tabular data (Fernández-Delgado et al., 2014; Grinsztajn et al., 2022; Kaggle, 2022; Uddin & Lu, 2024), while also offering practical advantages: they naturally handle both continuous and categorical features, require minimal hyperparameter tuning, and are substantially more computationally efficient than deep learning models (Grinsztajn et al., 2022). The strong empirical performance of RFs has been established in centralized settings, where data are assumed to be pooled together. However, this assumption is often unrealistic in many real-world applications, particularly in healthcare, where data are distributed across multiple institutions and cannot be centralized due to privacy regulations, governance constraints, or competitive considerations (Rieke et al., 2020; Antunes et al., 2022; Nguyen et al., 2022; Xu et al., 2021). Federated learning (FL) addresses this challenge by enabling collaborative model training on decentralized data (Kairouz et al., 2021). In this work, we focus on the standard server–client architecture and on horizontal FL, where clients hold disjoint sets of records described by a common feature space.

Federating random forests presents challenges fundamentally different from those of parametric models, whose training can be federated by aggregating parameters or gradients across clients (see e.g., FedAvg McMahan et al., 2017). In contrast, RFs are nonparametric and fully data-adaptive: each observation affects not only impurity values at each node but also the set of candidate split thresholds, which depend on the ordered feature values. Moreover, tree construction is inherently greedy and sequential, relying on hard, discontinuous splits; consequently, no gradients are available for aggregation across clients. To faithfully reproduce centralized behavior, impurity-based split decisions must be computed and updated using only aggregated client information, while respecting the sequential dependencies and without ever sharing raw data. This is made especially challenging by the heterogeneity of data across clients inherent to the federated setting: clients may differ in sample sizes, covariate distributions, or outcome mechanisms, and greedy split selection is highly sensitive to such differences. As a result, naive approaches—such as assembling locally trained forests or aggregating local split scores—can deviate substantially from centralized behavior.

¹Inria PreMeDiCaL, Inserm, University of Montpellier, France
²Sorbonne Université and Université Paris Cité, CNRS, Laboratoire de Probabilités, Statistique et Modélisation, F-75005 Paris.
 Correspondence to: Rémi Khellaf <remi.khellaf@inria.fr>.

Related work. A recent survey by Wang & Gai (2024) identifies three key challenges in decentralized training of tree-based models: computing split statistics without leaking sensitive information, limiting communication costs, and handling client heterogeneity.

Decision tree-based federated learning has mostly focus on gradient-boosted decision trees (GBDTs), which federate training by aggregating histogram-based gradient statistics (Ke et al., 2017; Li et al., 2023) or by sequentially fitting local trees to the residuals of a global model (Roth et al., 2022). GBDTs coordinate split selection using gradient information, whereas random forests provide no gradients and must rely on impurity-based, discrete split decisions. Moreover, boosted trees are inherently sequential in their construction: each tree depends on the residuals of all previous ones, and split selection typically requires full synchronization of clients at every node of every tree. In contrast, RFs are bagging-based, allowing trees to be constructed independently and in parallel—an important structural advantage in federated settings. Finally, federated GBDTs do not provide theoretical guarantees that the federated procedure reproduces the centralized greedy split objective.

Turning to federated RFs, early work focused on vertically partitioned data, using secure protocols for tree construction (Liu et al., 2020). In the horizontal setting we consider, most approaches are *local-ensemble* methods: clients train trees or forests locally, and the server either aggregates predictions (Liu et al., 2022) or subsamples local trees to form a global ensemble (Hauschild et al., 2022; Cotorobai et al., 2025; Xiang et al., 2024; Gu et al., 2023). These heuristics are best suited to approximately i.i.d. data; they neither explicitly accommodate small clients (since each local tree is fit on a reduced per-client sample) nor address covariate shift or client-specific feature–outcome relationships, and are therefore highly sensitive to client heterogeneity.

To the best of our knowledge, no prior work federates the CART split-selection step *itself* in horizontal FL while maintaining a clear link to the centralized greedy objective and accounting for realistic client-level data heterogeneity. The closest approach is Kalloori & Klingler (2022), which federates split selection by aggregating clients’ local histograms at each node. However, their method is heuristic: it approximates centralized CART through binning, offers no theoretical guarantees on split fidelity, and is not designed to handle covariate or outcome shifts, nor outlier data points.

Although RFs enjoy a substantial theoretical foundation in the centralized setting (Scornet et al., 2015), analogous guarantees are currently lacking for their federated counterparts. To pave the way toward provably reliable federated forests, we study the fundamental question of whether a federated split-selection mechanism can recover, or closely approximate, the greedy split decisions made by centralized CART.

Our contributions.

We propose a unified framework for federating CART decision trees and random forests that faithfully reproduces centralized training under realistic client heterogeneity without sharing individual data.

First, we introduce in Section 3.1 a **quantile-based candidate threshold generation** scheme and provide theoretical guarantees that it identifies the candidate closest to the split that would be selected by a centralized greedy CART. By estimating the pooled data distribution, defined as the mixture of the clients, this approach ensures that the threshold selection remains robust to client heterogeneity.

Next, we derive an **exact split-evaluation rule** (Section 3.2). We show that it reconstructs exactly the impurity gains that would result if all data were pooled, while relying solely on aggregated client statistics, thereby yielding decisions identical to the centralized CART algorithm. The key insight is that standard CART impurities admit additive sufficient statistics, which can be summed across clients to recover the centralized impurity—and hence the gain—exactly. We further design a **splitting rule on client indices** H , which our method allows to treat as a categorical feature with no extra communication. To our knowledge, this is the first method to explicitly support such splits, enabling a nonparametric form of personalization.

We emphasize the effect of heterogeneous data on greedy split selection, showing that impurity gains depend not only on feature–outcome relationships but also on covariate distributions. Consequently, adding a client with a different marginal $P(X)$ can change split decisions even when $P(Y | X)$ is shared across clients. We also **propose AvgImp, a more efficient approach for homogeneous regimes** (approximately i.i.d.), which aggregates local impurity gains and is supported by a finite-sample error bound.

Finally, we leverage the federated CART split-decision rule introduced above to develop our theoretically grounded *FedForest* method. Using standard random-forest randomization (client-stratified bootstrapping and feature subsampling), *FedForest* grows trees in parallel from aggregated client statistics alone, **recovering centralized-level predictive performance** with communication-efficient training.

We validate these findings through benchmarks on synthetic and real datasets in Section 5. Together, our results provide a practical, theory-backed framework for federating nonparametric trees and random forests under heterogeneous data and lay the foundation for federated extensions of other random forest variants, including quantile (Meinshausen & Ridgeway, 2006), survival (Ishwaran et al., 2008), and causal forests (Wager & Athey, 2018).

2. Problem Setting and Background

We consider a federated setting involving K clients collecting data described by the same set of features and addressing a supervised regression or classification task. Each client $k \in [K]$ holds a local dataset $\mathcal{D}_k = \{(H_i, X_i^{(k)}, Y_i^{(k)})\}_{i=1}^{n_k}$ consisting of n_k i.i.d. samples drawn from a d -dimensional distribution P_k , where the client indicator $H_i = k$ is constant within \mathcal{D}_k . The total sample size is $n = \sum_{k=1}^K n_k$.

Our goal is to learn a predictor $\hat{f} : \mathcal{X} \rightarrow \mathcal{Y}$ that performs well on the pooled population represented by the clients, i.e., the mixture distribution $P = \sum_{k=1}^K \rho_k P_k$ with weights $\rho_k = \mathbb{P}(H = k) \approx n_k/n$. More precisely, we aim to solve the following population optimization problem:

$$\min_{f \in \mathcal{F}} \mathcal{L}(f) = \sum_{k=1}^K \rho_k \mathbb{E}_{(X,Y) \sim P_k} [\ell(Y, f(X))], \quad (1)$$

where ℓ is the squared loss for regression and the 0–1 loss for classification.

2.1. Centralized CART/RF Split Selection

The mixture-risk objective (1) is an ideal target. CART and Random Forests approximate it through greedy, node-wise optimization of an impurity criterion (variance for regression; Gini or entropy for classification) on a finite data sample. In the centralized setting, all data are pooled as $\mathcal{D} = \bigcup_{k=1}^K \mathcal{D}_k$. At a node $\nu \subseteq \mathcal{X}$ of a tree, let $\mathcal{S}_\nu \subseteq \mathcal{D}$ be the samples reaching ν . CART selects a *split threshold* (j, t) —that is, a split variable $j \in [d]$ and a cutpoint $t \in \mathbb{R}$ —in two steps: (i) *candidate generation*, where for each feature j the values $\{x_{i,j}\}_{i \in \mathcal{S}_\nu}$ are sorted, and candidates t are defined as the midpoints between consecutive distinct values; and (ii) *split evaluation*, where each candidate (j, t) is scored by its empirical impurity reduction

$$\Delta I(j, t; \mathcal{S}_\nu) = I(\mathcal{S}_\nu) - \left(\frac{n_L}{n_\nu} I(\mathcal{S}_L) + \frac{n_R}{n_\nu} I(\mathcal{S}_R) \right), \quad (2)$$

with $\mathcal{S}_L = \{i \in \mathcal{S}_\nu : x_{i,j} \leq t\}$, $\mathcal{S}_R = \{i \in \mathcal{S}_\nu : x_{i,j} > t\}$, $n_L = |\mathcal{S}_L|$, $n_R = |\mathcal{S}_R|$, and $n_\nu = n_L + n_R$. CART then selects the threshold (j, t) that maximizes $\Delta I(j, t; \mathcal{S}_\nu)$.

Random Forests build an ensemble of CART trees, adding randomness through bootstrap sampling—each tree is trained on a different sample of \mathcal{D} —and feature subsampling at each node (typically \sqrt{d} for classification, $d/3$ for regression). Predictions are aggregated across trees by averaging in regression, or by majority vote in classification. In practice, individual trees are further regularized using standard stopping rules, such as maximum depth, minimum leaf size, or minimum impurity decrease.

In the federated setting, the pooled dataset is never accessible, and clients may only share aggregated summaries with the server. Existing federated tree methods largely restrict splits to X and lack a principled way to split on H . Our

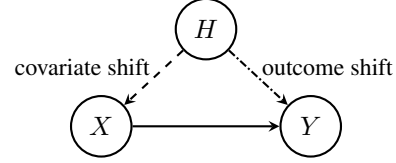


Figure 1. Graphical models of the heterogeneity regimes. Dashed arrows indicate possible dependencies between the client variable H and the covariates and/or outcome mechanism, depending on the regime.

goal is thus to reproduce centralized split selection from aggregated client statistics while enabling client-aware splits under heterogeneity.

2.2. Heterogeneity Scenarios

We formalize the data heterogeneity regimes considered in this work and relate each of them to the behavior of a centralized CART-based model trained on pooled data. Figure 1 shows the associated graphical models and highlights situations where the client variable H carries predictive information for the outcome Y .

General model. In full generality, the combined data admit the decomposition

$$P(X, Y, H) = P(Y | X, H) P(X | H) P(H), \quad (3)$$

which allows both the covariate distribution and the outcome mechanism to vary across clients. This formulation captures realistic scenarios in which institutions differ both in their underlying populations and in the relationship between features and outcomes. The three regimes below correspond to restrictions of (3).

Assumption 2.1 (Homogeneous setting). $(X, Y) \perp\!\!\!\perp H$.

In this scenario, all clients are drawn from the same population. Equivalently, $P(X | H) = P(X)$ and $P(Y | X, H) = P(Y | X)$. Pooling data only increases the effective sample size, while H carries no predictive information once X is observed. Consequently, splitting on H yields no (asymptotic) impurity reduction.

Assumption 2.2 (Covariate shift setting). $P(Y | X, H) = P(Y | X)$, while $P(X | H)$ may depend on H .

In this regime, clients differ in their populations but share the same outcome mechanism; in other words, there is no “client effect”. This implies that the conditional expectation of the outcome given features, $f(x) = \mathbb{E}[Y | X = x]$, is common to all clients, and therefore that H is not required for prediction once X is observed. However, the marginal feature distribution is a mixture $P(X) = \sum_{k=1}^K \rho_k P(X | H = k)$. As a result, clients may exhibit partially or even fully non-overlapping feature supports, so that the pooled

dataset covers regions of the input space that are under-represented or entirely absent in individual local datasets.

Assumption 2.3 (Outcome shift (client effect) setting). $P(X | H) = P(X)$ while $P(Y|X)$ may depend on H .

In this setting, the conditional relationship of outcomes given the covariates may depend on the client. Conditioning on X alone is generally insufficient: the optimal prediction rule is $f(x, h) = \mathbb{E}[Y | X = x, H = h]$. Equivalently, H induces an effect on Y and must be included in the conditioning set. A centralized CART/RF trained on pooled data can capture this structure by treating H as an input feature and splitting on it whenever it reduces impurity.

3. Federated CART

In this section, we present our approach for reproducing CART’s split selection in the federated setting. At any node ν , let $\mathcal{S}_{\nu,k}$ denote the subset of $n_{\nu,k}$ samples from client k that reach ν . The pooled node sample exists only as the virtual union $\mathcal{S}_\nu = \bigcup_{k=1}^K \mathcal{S}_{\nu,k}$. Our federated split selection rule has two key components: (i) constructing a finite set of candidate splits from distributed information (Section 3.1); and (ii) evaluating each candidate’s impurity reduction using only client-to-server summaries (Section 3.2).

3.1. Candidate Split Generation

In centralized CART implementations (e.g., `scikit-learn` Pedregosa et al., 2011), the pooled values $\{x_{i,j}\}_{i \in \mathcal{S}_\nu}$ are sorted, and all midpoints between consecutive distinct values of each feature j are evaluated. While exact, this midpoint grid is impractical in the federated setting, as it would require communicating essentially all node-level feature values.

Naive alternatives are also unsatisfactory under client heterogeneity: fixed grids depend on feature scaling and can miss narrow high-gain regions, while random grids provide no guarantees and may miss low-density gaps between client supports under covariate shift. Instead, we propose *federated quantile sketching*: a data-adaptive, communication-efficient candidate-generation scheme that estimates the pooled (mixture) distribution at node ν from aggregated client summaries, and remains reliable under covariate shift, including disjoint client supports.

Federated quantile sketching. We construct a compact candidate set based on pooled quantiles. For each continuous feature j and node ν , client k computes B empirical quantiles $\mathbf{q}_{\nu,k}^{(j)} = (q_{\nu,k,1}^{(j)}, \dots, q_{\nu,k,B}^{(j)})$ on its node data $\mathcal{S}_{\nu,k}$, and sends them to the server. The server converts $\mathbf{q}_{\nu,k}^{(j)}$ into a piecewise-linear approximation $\tilde{F}_{\nu,k}^{(j)}$ of the local empirical cumulative distribution functions (CDF) $F_{\nu,k}^{(j)}$, and then

constructs a pooled CDF estimate via a mixture:

$$\tilde{F}_\nu^{(j)}(x) = \sum_{k=1}^K \frac{n_{\nu,k}}{n_\nu} \tilde{F}_{\nu,k}^{(j)}(x), \quad (4)$$

with $n_\nu = \sum_{k=1}^K n_{\nu,k}$. Finally, candidate thresholds are selected as the interior quantiles of the reconstructed pooled CDF:

$$\mathcal{T}_\nu^{(j)} = \left\{ (\tilde{F}_\nu^{(j)})^{-1}\left(\frac{b}{B}\right) : b = 1, \dots, B-1 \right\}.$$

Importantly, we do not average local quantiles (which in general does not yield pooled quantiles); instead we aggregate CDF sketches and invert the pooled CDF.

Theorem 3.1 (Uniform rank error of the reconstructed CDF). *Let $F_\nu^{(j)}(x) = \sum_{k=1}^K \frac{n_{\nu,k}}{n_\nu} F_{\nu,k}^{(j)}(x)$ be the pooled empirical CDF for feature j at node ν , and let $\tilde{F}_\nu^{(j)}$ be obtained by linearly interpolating between the B reported quantile points per client and mixing as above. Then,*

$$\sup_x |\tilde{F}_\nu^{(j)}(x) - F_\nu^{(j)}(x)| \leq \frac{1}{B}.$$

Corollary 3.2 (Approximation of centralized midpoint splits). *Let $\mathcal{T}_{\text{cent}}$ denote the centralized midpoint candidates at node ν , and let $\mathcal{T}_{\text{fed}} = \bigcup_{j=1}^d \{(j, t) : t \in \mathcal{T}_\nu^{(j)}\}$ be the quantile-based grid. For any $(j, t_{\text{cent}}) \in \mathcal{T}_{\text{cent}}$, there exists $(j, t_{\text{fed}}) \in \mathcal{T}_{\text{fed}}$ such that the induced left-child assignments disagree on at most a $\frac{3}{2B}$ fraction of pooled samples:*

$$\frac{1}{n_\nu} \sum_{i \in \mathcal{S}_\nu} \mathbb{1}(\mathbb{1}(x_{i,j} \leq t_{\text{cent}}) \neq \mathbb{1}(x_{i,j} \leq t_{\text{fed}})) \leq \frac{3}{2B}.$$

Theorems 3.1 and 3.2 (proved in Appendix A.3) show that B directly controls the rank resolution of the candidate grid: increasing B makes the federated quantile thresholds closer to the centralized midpoint thresholds in terms of induced child assignments. For example, setting $B = 100$ percentiles implies at most 1.5% disagreement in child assignments while requiring only $B - 1$ candidates per feature, independent of n_ν . These results allow precise control of the trade-off between communication cost and candidate-threshold fidelity to the centralized approach.

Our quantile-based candidates are superior to the fixed-width histograms proposed by Kalloori & Klingler (2022) for three reasons: (i) they adapt to local data density, ensuring critical split points are preserved as well as possible for a given budget B ; (ii) they are more robust against outliers; and (iii) they mitigate privacy leakage by enforcing a minimum sample fraction of $1/B$ within each bin.

Top- L feature shortlisting for homogeneous data. Under Theorem 2.1, local impurity gains concentrate around the pooled gain, so local rankings tend to agree with the

global ranking. This enables a communication-efficient pre-selection step before candidate generation: each client k computes, for each feature j , its best local gain

$$M_{\nu,k}(j) = \max_t \Delta I(j, t; \mathcal{S}_{\nu,k}),$$

and sends only its top- L features (with associated gains). The server merges these reports (e.g., taking the union of the local top- L sets) to form a reduced feature set \mathcal{L}_ν on which it performs quantile sketching and split evaluation. A supporting guarantee for retaining the pooled-best feature under Theorem 2.1 is given in Appendix A.4.1.

Discrete features. For small-cardinality categorical variables, clients can send exact category counts and the server evaluates all admissible splits with negligible cost. For high-cardinality categories, we use the standard ordering trick known as Fisher grouping (Fisher, 1958): we order categories by their within-node outcome mean (regression) or class proportion (binary classification), treat the ordered categories as an ordinal feature, and scan contiguous splits.

3.2. Federated Impurity Reduction

Given the candidate set from Section 3.1, the remaining step is to evaluate the impurity reduction (2) for each candidate split (j, t) without exchanging raw data subsets. Our main evaluation rule is based on a novel observation: standard CART impurities admit *additive sufficient statistics* that can be aggregated across clients to recover the centralized impurity exactly.

Exact centralized evaluation via additive summaries. For standard CART criteria, there exists a deterministic map Ψ and per-client summaries $\mathbf{s}_{\nu,k}$ such that the pooled impurity reduction can be written as

$$\Delta I(j, t; \mathcal{S}_\nu) = \Psi(\mathbf{s}_\nu) - \left(\frac{n_L}{n_\nu} \Psi(\mathbf{s}_L) + \frac{n_R}{n_\nu} \Psi(\mathbf{s}_R) \right), \quad (5)$$

with aggregated statistics $\mathbf{s}_m = \sum_{k=1}^K \mathbf{s}_{m,k}$ for $m \in \{\nu, L, R\}$. In practice, for a candidate (j, t) , each client sends only its left-child summary $\mathbf{s}_{L,k}$; the server aggregates \mathbf{s}_L , recovers $\mathbf{s}_R = \mathbf{s}_\nu - \mathbf{s}_L$, and evaluates (5). This matches centralized split evaluation exactly, regardless of covariate shift or outcome heterogeneity.

Examples. For C -class classification, $\mathbf{s}_\nu = (n_{\nu,1}, \dots, n_{\nu,C})$, $\Psi_{\text{Gini}}(\mathbf{s}_\nu) = 1 - \sum_{c=1}^C (n_{\nu,c}/n_\nu)^2$, so each client sends C scalars per candidate. For regression, $\mathbf{s}_\nu = (n_\nu, S_\nu, Q_\nu)$ with $S_\nu = \sum y_i$, $Q_\nu = \sum y_i^2$, $\Psi_{\text{Var}}(\mathbf{s}_\nu) = Q_\nu/n_\nu - (S_\nu/n_\nu)^2$, so each client sends 3 scalars.

The following theorem justifies the above strategy by showing that aggregating local impurities generally fails to recover the global impurity, introducing an additional error term.

Theorem 3.3 (General impurity decomposition). *Let $I(\mathcal{S}_\nu)$ denote the empirical impurity at node ν . Then*

$$I(\mathcal{S}_\nu) = \sum_{k=1}^K \frac{n_{\nu,k}}{n_\nu} I(\mathcal{S}_{\nu,k}) + \mathcal{E}(\nu), \quad (6)$$

where $\mathcal{E}(\nu)$ is a heterogeneity (Jensen-gap) term induced by the within-node mixture of client distributions. For standard strictly concave impurity functions (e.g., Gini index, entropy, variance), we have $\mathcal{E}(\nu) \geq 0$, with $\mathcal{E}(\nu) = 0$ if and only if

$$\forall(k, k'), \quad \hat{\mathbb{E}}[Y \mid \mathcal{S}_\nu, H = k] = \hat{\mathbb{E}}[Y \mid \mathcal{S}_\nu, H = k'],$$

i.e., the within-node empirical outcome means (or class probabilities) coincide across all clients.

The term $\mathcal{E}(\nu)$ explains why split decisions based solely on local objectives can deviate from the centralized CART choice when clients are heterogeneous.

Cheaper approximation based on averaging local gains (AvgImp). While the decomposition above highlights risks in heterogeneous settings, it also suggests a faster alternative for homogeneous regimes (Theorem 2.1). When $\mathcal{E}(\nu) \approx 0$, the global gain can be approximated by the weighted average of local gains:

$$\widehat{\Delta I}_{\text{AvgImp}}(j, t; \mathcal{S}_\nu) := \sum_{k=1}^K \frac{n_{\nu,k}}{n_\nu} \Delta I(j, t; \mathcal{S}_{\nu,k}).$$

This proxy motivates our *AvgImp* strategy: a conjunction of (i) local Top- L screening—where each client proposes only its best candidates based on local gains—and (ii) an evaluation based on the averaged metric above. This approach drastically reduces communication by avoiding the evaluation of all pooled candidates.

Theorem 3.4 (*AvgImp* approximation error on homogeneous data). *Under Theorem 2.1 and $\mathbb{E}[Y^2] < \infty$,*

$$\left| \widehat{\Delta I}_{\text{AvgImp}}(j, t; \mathcal{S}_\nu) - \Delta I(j, t; \mathcal{S}_\nu) \right| = O_p\left(\frac{K}{n_\nu}\right).$$

In summary, (5) is our primary evaluation rule (exact centralized gain), while Theorem 3.3–Theorem 3.4 motivate *AvgImp* as a communication-lean approximation that is accurate when data is (close to) homogeneous.

Outcome shift: splitting on H with no extra communication. Under Theorem 2.3, the target rule is $f(x, h) = \mathbb{E}[Y \mid X = x, H = h]$, and optimal trees may require splits on H . Let $\mathcal{K}_\nu = \{k : n_{\nu,k} > 0\}$ be the set of active clients at node ν . Once the server has collected the per-client node summaries $\{\mathbf{s}_{\nu,k}\}_{k \in \mathcal{K}_\nu}$ —already needed to evaluate feature-based splits—it can also evaluate splits on H at no additional communication cost, i.e., without

requesting any extra messages from clients. Indeed, any partition $\mathcal{K}_\nu = \mathcal{K}_L \cup \mathcal{K}_R$ induces

$$\mathbf{s}_{\nu,L} = \sum_{k \in \mathcal{K}_L} \mathbf{s}_{\nu,k} \quad \text{and} \quad \mathbf{s}_{\nu,R} = \sum_{k \in \mathcal{K}_R} \mathbf{s}_{\nu,k},$$

and the corresponding gain follows directly from (5) using the same map Ψ .

Although there are $2^{|\mathcal{K}_\nu|-1}$ partitions, the optimal split can be found efficiently: for regression and binary classification, it suffices to sort sites by their within-node means $\bar{y}_{\nu,k}$ and scan contiguous splits (Fisher, 1958), for a cost $O(|\mathcal{K}_\nu| \log |\mathcal{K}_\nu|)$. When H has many categories, treating H -splits as Fisher groupings is essential; otherwise trees waste depth constructing arbitrary partitions of client IDs.

4. Federated Forests

We now describe how to transform the federated split primitives of Section 3—candidate generation and split evaluation from summaries—into a scalable Random Forest training protocol, which we call *FedForest*. The key ingredients are: (i) local bootstrap resampling to introduce tree-level randomness while preserving the pooled mixture, (ii) per-node feature subsampling and (optional) Top- L shortlisting to limit the number of feature–threshold pairs evaluated, and (iii) level-wise batching to train many trees in a small number of synchronized communication rounds.

4.1. Bootstrap and Client Subsampling

Client-stratified bootstrap. For each tree, client k draws (with replacement) a bootstrap sample of size n_k from \mathcal{D}_k and the tree is trained on the virtual union of these resamples across clients. This preserves the pooled mixture weights $\rho_k = n_k/n$ in every tree. In contrast, a pooled bootstrap can under-represent—or entirely omit—small clients.

Client subsampling. For a given tree (or node), the server can a client subset $\mathcal{K}' \subseteq [K]$ to reduce communication. We recommend it mainly as an acceleration knob under approximately homogeneous clients: under covariate shift, it changes the effective mixture distribution and may alter split decisions, and under outcome shift it can also omit informative values of H .

4.2. Parallel tree growth and batched rounds

Tree growth is sequential *within* a tree, but independent *across* trees given the local bootstrap and feature subsampling. We exploit this by training all trees level-wise: at a given depth, the server batches the active nodes across all trees into a single request, clients answer for the whole batch in one message, and the server updates all nodes independently. As a result, training T trees to depth M requires $O(M)$ synchronized rounds (rather than scaling with the

total number of nodes). This batching is also compatible with client-side parallelism, since node computations are embarrassingly parallel across ν .

4.3. FedForest Training Protocol

We summarize the complete server–client protocol for training a forest with T trees of depth at most M in Algorithm 1. Each node ν is identified by its path from the root and the tree index; each client can therefore compute the set of local samples reaching ν without sharing indices.

Algorithm 1 FEDFOREST (Quantiles + Fisher for H)

- 1: **Input:** #trees T , depth M , subsample r , sketch size B .
 - 2: **Output:** Forest predictor \hat{f} .
 - 3: **Init:** Server selects client subsets \mathcal{K}_τ (size $\lceil rK \rceil$); Clients draw bootstrap samples.
 - 4: Server initializes root nodes $\mathcal{A} = \{(\tau, \text{root})\}_{\tau=1}^T$.
 - 5: **for** $\ell = 0$ **to** $M - 1$ **do**
 - 6: **Server:** Broadcasts previous split decisions and selects features \mathcal{J}_ν for active nodes $\nu \in \mathcal{A}$.
 - 7: **Clients (Parallel):** For all τ and $k \in \mathcal{K}_\tau$:
 - 8: Update local node membership for active nodes ν .
 - 9: Compute sketches $\mathbf{q}_{\nu,k}^{(j)}$ for continuous $X \in \mathcal{J}_\nu$.
 - 10: Compute local node summaries $\mathbf{s}_{\nu,k}$ (for H).
 - 11: Send sketches and summaries to Server.
 - 12: **Server (Candidate Generation):**
 - 13: **For** X : Aggregate sketches \rightarrow approximate pooled CDF via Equation (4) \rightarrow candidates $\mathcal{T}_\nu^{(X)}$.
 - 14: **For** H : Compute site means from $\mathbf{s}_{\nu,k}$; sort site indices σ by mean; generate splits $\mathcal{T}_\nu^{(H)}$.
 - 15: Broadcast candidates $\mathcal{T}_\nu = \mathcal{T}_\nu^{(X)} \cup \mathcal{T}_\nu^{(H)}$.
 - 16: **Clients (Parallel):** For all τ and $k \in \mathcal{K}_\tau$:
 - 17: Compute **left-child summaries** $\mathbf{s}_{L,k}(j, t)$ for all candidates $(j, t) \in \mathcal{T}_\nu$.
 - 18: Send to Server.
 - 19: **Server:** Aggregates $\mathbf{s}_L = \sum_k \mathbf{s}_{L,k}$; evaluates impurity gain via Equation (5);
 - 20: Selects best split (j^*, t^*) and updates \mathcal{A} .
 - 21: **end for**
 - 22: **Finalize:** Server computes leaf values from final node summaries.
-

Communication per node. We count communication in transmitted scalars for one node ν and one client k , with d active features, B quantile levels (sketch size), and sufficient-statistic size S (e.g., $S = 3$ for regression and $S = C$ for C -class classification). All costs below are independent of the node sample sizes $(n_{\nu,k}, n_\nu)$.

FedForest (exact gain). Communication has two steps. (i) Sketching: the client sends d univariate quantile sketches of size B , for a cost dB . (ii) Evaluation: for each tested threshold in \mathcal{T} , the client returns the left-child sufficient

statistics, costing S scalars per candidate. So the total cost of FedForest per node is $O(dBS)$.

Top-L shortlisting. If the server evaluates only $|\mathcal{L}_\nu| \ll d$ shortlisted features, the evaluation term becomes $|\mathcal{L}_\nu|BS$.

AvgImp (Top-L + averaged local gains). If clients compute their impurity gains locally at the candidate thresholds of the shortlisted features, they send *one scalar per threshold* instead of S . Combining Top-L with AvgImp therefore reduces the evaluation communication to $|\mathcal{L}_\nu|B$, at the price of shifting computation from the server to the clients for the local gain evaluation.

5. Experiments

5.1. Synthetic Data

Experimental setting. We simulate an horizontal multicenter setting with K clients, where the k -th client holds n_k i.i.d. samples $(H_i = k, X_i^{(k)}, Y_i^{(k)})$. Covariates are drawn from client-specific Gaussians $X_i^{(k)} \sim \mathcal{N}(\mu_k, \alpha_k I_d)$, with $\mu_k = [(-1)^k \gamma, \dots, (-1)^k \gamma]$, $\gamma \geq 0$ and $\alpha_k > 0$. The separation between client distribution can be tuned via γ and α_k . Choosing a small values for γ and large values for α_k corresponds to client distributions with large overlaps. Observed outcomes are generated as $Y_i^{(k)} = f(X_i^{(k)}) + \delta_k + \varepsilon_i$, where $\varepsilon_i \sim \mathcal{N}(0, \sigma^2)$ is an independent noise, $\delta_k = (-1)^k \delta$ is a client-specific shift controlling outcome heterogeneity, where the function f is a decision-tree function (see Section D). We compare our proposed methods to several federated baselines and a centralized RF, considered as the reference as it is trained on pooled data (via `scikit-learn`, see Pedregosa et al., 2011). Federated baselines include:

1. Federated Histogram (Kalloori & Klingler, 2022), adapted to regression via node-wise sufficient statistics for squared error (counts, sums, sums of squares);
2. One-shot local ensembling (Hauschild et al., 2022), where clients train local forests and the server aggregates predictions;
3. Local learning, where each client trains on \mathcal{D}_k only.

We compare these competitors to our proposed methods:

1. FedForest-Quantiles, which uses quantile sketches to propose candidate thresholds and exact split evaluation via additive sufficient statistics;
2. FedForest-AvgImp/Top-L, our cheaper variant that shortlists features using Top-L and evaluates candidates using averaged local impurity gains.

All RFs use $T = 50$ trees, with a maximum depth of 8, a minimum leaf size of 5, feature subsampling \sqrt{d} , and client-stratified bootstrapping. For candidate generation,

FedForest methods and Federated Histogram use $B = 32$ candidates per feature, and the FedForest AvgImp method screens $L = 3$ features.

In our methods, H is always included as a split candidate (i.e., not subject to feature subsampling) so that the model can capture client effects when they reduce impurity. Baselines that do not implement client splits are evaluated on X only. Whereas not natively supported for regression RFs, using Fisher’s encoding of the client indicator improves the predictive performance of centralized RFs that allow splits on H . We use such encoding at the root node for centralized RFs, while our method recomputes this encoding at every node based on the shared node summaries.

We consider $K = 10$ clients holding $d = 20$ features, and $n_k = 200$ samples per client, with the three settings:

1. **(Homogeneous)** $\forall k \in [K], \gamma_k = \delta = 0$ and $\alpha_k = 1$;
2. **(Covariate shift)** $\forall k \in [K], \gamma_k = 3$ and $\alpha_k = 0.5$;
3. **(Outcome shift)** $\delta = 1.5, \forall k \in [K], \alpha_k = 1$ and $\gamma_k = 0$ (homogeneous covariates).

Results. Figure 2 reports, in the homogeneous setting, the test mean squared error (MSE) on a 30% held-out set drawn from the client mixture, averaged over 150 synthetic data generations. Here, our proposed FedForest Quantiles (regardless of including H as a splitting variable) and Federated Histogram (which does not use H for splitting) are comparable to the centralized RF. FedForest without including H exhibits a lower variance than Federated Histogram. Local methods (either local learning or local ensembling), which are built independently on each client, perform poorly, due to the smaller effective sample size per client. Indeed, while no bias is expected from local learning in this setting, each tree is trained on less data compared to other federated or centralized methods. Our approximate variant FedForest AvgImp (averaging impurity gains) performs slightly less well, and worsens when H is included; with larger candidate grids B or more screened features L , it reaches centralized RF performance.

In the covariate shift scenario (Figure 3), the chosen (γ_k, α_k) yield a shift close to disjoint client supports, and we design the outcome to require a split near 0 between these supports, making this an extreme regime that clearly exposes flawed procedures. As in the homogeneous case, FedForest Quantiles (with or without H) and Federated Histograms are competitive with centralized RF. FedForest AvgImp performs poorly, as expected outside its intended (approximately i.i.d.) regime: with disjoint supports, averaging clientwise impurity gains can miss splits *between* supports because each client’s impurity reduction is then zero (all its samples fall on one side). Allowing AvgImp to split on H improves performance since H acts as a proxy for identifying the support of the client distribution. On

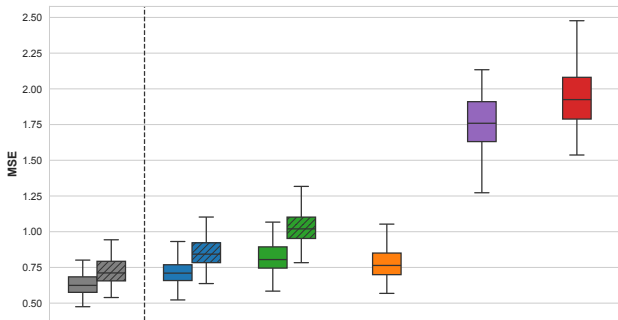


Figure 2. Methods comparison on homogeneous clients

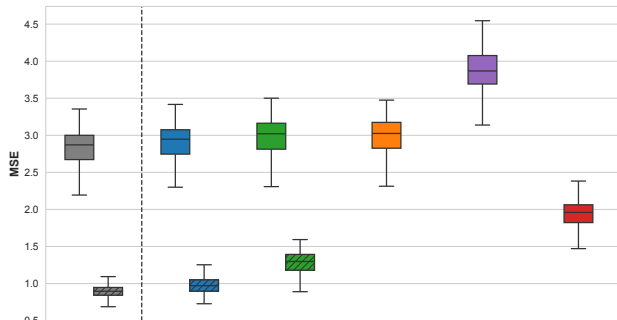


Figure 4. Methods comparison under outcome shift

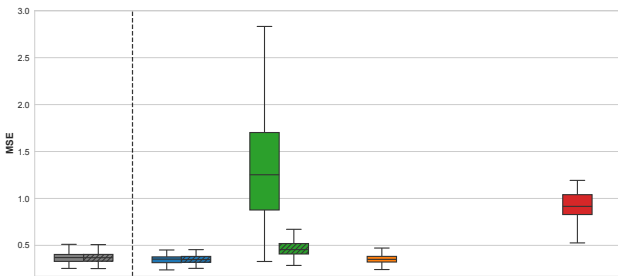


Figure 3. Methods comparison under covariate shift

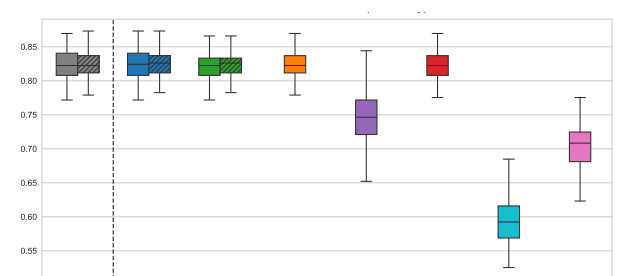


Figure 5. Methods comparison on FedHeart-Disease dataset

the contrary, methods that select the best split based on an impurity reduction computed with a mixture of all client data (as centralized RF or the three federated methods mentioned above) succeed in detecting relevant splits, even when H is not added as a covariate, thus having good predictive performances. Local ensembling is not reported due to its extremely high MSE (≈ 141.2), reflecting its inability to handle covariate shift. When client data supports are disjoint, trees are trained independently on each client, and the random forest averages predictions from many irrelevant trees, as a tree trained on one client typically produces near-constant predictions on data from other clients.

Finally, Figure 4 (outcome shift) highlights the benefit of client-aware structure: including H substantially improves performance for methods that can split on H (centralized and our FedForest variants), whereas baselines restricted to X cannot capture client effects and incur a larger error. Note that Federated Histograms are not designed to split on H so they fail in this context.

5.2. Real Data

We further validate our approach on the FedHeart Disease dataset of the Flamby federated benchmark (Ogier du Terrail et al., 2022), a binary classification task involving 740 patients and 13 clinical covariates distributed across four in-

stitutions in the USA (Cleveland, Long Beach), Switzerland, and Hungary. To provide a comprehensive benchmark, we compare our method against two standard federated baselines established in Ogier du Terrail et al. (2022): (i) **FedAvg LR**, a logistic regression model trained collaboratively with FedAvg (McMahan et al., 2017); and (ii) **FedAvg NN**, a non-linear two-layer neural network trained via Federated Averaging. Notably, we observe that our methods FedForest Quantiles and FedForest AvgImp have good predictive performances, together with Federated Histograms and Local Learning. Neural networks and Logistic regression fail here. This highlights that Federated Random Forests (FedForest, Federated Histograms, or local learning) outperform these federated parametric models, highlighting the critical importance of flexible, non-linear modeling in this heterogeneous regime.

6. Conclusion

We propose *FedForest*, a federated forests procedure with formal guarantees, proving that centralized CART and RF behavior can be exactly recovered from federated data. Our approach serves as a foundational building block for extending the entire family of CART-criterion-based methods, including causal, quantile, and survival Forests, to heterogeneous federated environments.

Impact Statement

This paper presents work whose goal is to advance the field of machine learning. There are many potential societal consequences of our work, none of which we feel must be specifically highlighted here.

References

- Antunes, R. S., André da Costa, C., Küderle, A., Yari, I. A., and Eskofier, B. Federated learning for healthcare: Systematic review and architecture proposal. *ACM Transactions on Intelligent Systems and Technology (TIST)*, 13(4):1–23, 2022.
- Breiman, L. Random forests. *Machine learning*, 45(1): 5–32, 2001.
- Breiman, L., Friedman, J. H., Olshen, R. A., and Stone, C. J. *Classification and Regression Trees*. Wadsworth, Monterey, CA, 1984.
- Cotorobai, A., Silva, J. M., and Oliveira, J. L. A federated random forest solution for secure distributed machine learning. *arXiv preprint arXiv:2505.08085*, 2025.
- Fernández-Delgado, M., Cernadas, E., Barro, S., and Amorim, D. Do we need hundreds of classifiers to solve real world classification problems? *The journal of machine learning research*, 15(1):3133–3181, 2014.
- Fisher, W. D. On grouping for maximum homogeneity. *Journal of the American statistical Association*, 53(284): 789–798, 1958.
- Grinsztajn, L., Oyallon, E., and Varoquaux, G. Why do tree-based models still outperform deep learning on typical tabular data? In Koyejo, S., Mohamed, S., Agarwal, A., Belgrave, D., Cho, K., and Oh, A. (eds.), *Advances in Neural Information Processing Systems 35: Annual Conference on Neural Information Processing Systems 2022, NeurIPS 2022, New Orleans, LA, USA, November 28 - December 9, 2022*, 2022.
- Gu, T., Lee, P. H., and Duan, R. COMMUTE: Communication-efficient transfer learning for multi-site risk prediction. *Journal of Biomedical Informatics*, 137: 104243, 2023.
- Hauschild, A.-C., Lemanczyk, M., Matschinske, J., Frisch, T., Zolotareva, O., Holzinger, A., Baumbach, J., and Heid²er, D. Federated random forests can improve local performance of predictive models for various healthcare applications. *Bioinformatics*, 38(8):2278–2286, 2022.
- Ishwaran, H., Kogalur, U. B., Blackstone, E. H., and Lauer, M. S. Random survival forests. 2008.
- Kaggle. 2022 Kaggle Machine Learning & Data Science Survey, 2022. URL <https://www.kaggle.com/c/kaggle-survey-2022>.
- Kairouz, P., McMahan, H. B., Avent, B., Bellet, A., Bennis, M., Bhagoji, A. N., Bonawitz, K., Charles, Z., Cormode, G., Cummings, R., et al. Advances and open problems in federated learning. *Foundations and trends® in machine learning*, 14(1–2):1–210, 2021.
- Kalloori, S. and Klingler, S. Cross-silo federated learning based decision trees. In *Proceedings of the 37th ACM/SIGAPP Symposium on Applied Computing*, pp. 1117–1124, 2022.
- Ke, G., Meng, Q., Finley, T., Wang, T., Chen, W., Ma, W., Ye, Q., and Liu, T.-Y. Lightgbm: A highly efficient gradient boosting decision tree. *Advances in neural information processing systems*, 30, 2017.
- Li, Q., Wu, Z., Cai, Y., Yung, C. M., Fu, T., and He, B. FedTree: A federated learning system for trees. In *Proceedings of Machine Learning and Systems*, volume 5, 2023.
- Liu, S., Wang, J., and Zhang, W. Federated personalized random forest for human activity recognition. *Mathematical Biosciences and Engineering*, 19(1):953–971, 2022.
- Liu, Y., Liu, Y., Liu, Z., Liang, Y., Meng, C., Zhang, J., and Zheng, Y. Federated forest. *IEEE Transactions on Big Data*, 8(3):843–854, 2020.
- McMahan, B., Moore, E., Ramage, D., Hampson, S., and y Arcas, B. A. Communication-efficient learning of deep networks from decentralized data. In *Artificial intelligence and statistics*, pp. 1273–1282. PMLR, 2017.
- Meinshausen, N. and Ridgeway, G. Quantile regression forests. *Journal of machine learning research*, 7(6), 2006.
- Nguyen, D. C., Pham, Q.-V., Pathirana, P. N., Ding, M., Seneviratne, A., Lin, Z., Dobre, O., and Hwang, W.-J. Federated learning for smart healthcare: A survey. *ACM Computing Surveys (Csur)*, 55(3):1–37, 2022.
- Ogier du Terrail, J., Ayed, S.-S., Cyffers, E., Grimberg, F., He, C., Loeb, R., Mangold, P., Marchand, T., Marfoq, O., Mushtaq, E., et al. Flamby: Datasets and benchmarks for cross-silo federated learning in realistic healthcare settings. *Advances in Neural Information Processing Systems*, 35:5315–5334, 2022.
- Pedregosa, F., Varoquaux, G., Gramfort, A., Michel, V., Thirion, B., Grisel, O., Blondel, M., Prettenhofer, P., Weiss, R., Dubourg, V., Vanderplas, J., Passos, A., Cournapeau, D., Brucher, M., Perrot, M., and Duchesnay, E. Scikit-learn: Machine learning in Python. *Journal of Machine Learning Research*, 12:2825–2830, 2011.

- Rieke, N., Hancox, J., Li, W., Milletari, F., Roth, H. R., Albarqouni, S., Bakas, S., Galtier, M. N., Landman, B. A., Maier-Hein, K., et al. The future of digital health with federated learning. *NPJ digital medicine*, 3(1):119, 2020.
- Roth, H. R., Cheng, Y., Wen, Y., Yang, I., Xu, Z., Hsieh, Y., Kersten, K., Harouni, A., Zhao, C., Lu, K., et al. Nvidia flare: Federated learning from simulation to real-world. *arXiv preprint arXiv:2210.13291*, 2022.
- Scornet, E., Biau, G., and Vert, J.-P. Consistency of random forests. 2015.
- Uddin, S. and Lu, H. Confirming the statistically significant superiority of tree-based machine learning algorithms over their counterparts for tabular data. *PLOS ONE*, 19(4):1–12, 04 2024. doi: 10.1371/journal.pone.0301541. URL <https://doi.org/10.1371/journal.pone.0301541>.
- Wager, S. and Athey, S. Estimation and inference of heterogeneous treatment effects using random forests. *Journal of the American Statistical Association*, 113(523):1228–1242, 2018.
- Wang, Z. and Gai, K. Decision tree-based federated learning: A survey. *Blockchains*, 2(1):40–60, 2024.
- Xiang, P., Zhou, L., and Tang, L. Transfer learning via random forests: A one-shot federated approach. *Computational Statistics & Data Analysis*, 197:107975, 2024.
- Xu, J., Glicksberg, B. S., Su, C., Walker, P., Bian, J., and Wang, F. Federated learning for healthcare informatics. *Journal of healthcare informatics research*, 5(1):1–19, 2021.

A. Proofs

A.1. Impurity Decomposition

Proof of Theorem 3.3 which states:

$$I(\mathcal{S}_\nu) = \sum_{k=1}^K \frac{n_{\nu,k}}{n_\nu} I(\mathcal{S}_{\nu,k}) + \mathcal{E}(\nu),$$

where the heterogeneity term $\mathcal{E}(\nu)$ is:

$$\mathcal{E}(\nu) = \Psi \left(\sum_{k=1}^K \frac{n_{\nu,k}}{n_\nu} \hat{P}_k \right) - \sum_{k=1}^K \frac{n_{\nu,k}}{n_\nu} \Psi(\hat{P}_k),$$

where \hat{P}_k is the empirical distribution of client k 's outcome and Ψ is the impurity function from statistics, and for variance, Gini and entropy impurity functions we have $\mathcal{E}(\nu) \geq 0$ and:

$$\mathcal{E}(\nu) = 0 \iff \forall(k, k'), \mathbb{E}[Y | X, \mathcal{S}_\nu, H = k] = \mathbb{E}[Y | X, \mathcal{S}_\nu, H = k'].$$

Proof. Let \mathcal{S}_ν be the set of samples at node ν , and $\mathcal{S}_{\nu,k}$ the subset of samples belonging to client k , such that $\mathcal{S}_\nu = \bigcup_{k=1}^K \mathcal{S}_{\nu,k}$ and $\mathcal{S}_{\nu,k} \cap \mathcal{S}_{\nu,k'} = \emptyset$. Let P_ν denote the empirical distribution of the target variable Y over the pooled sample \mathcal{S}_ν , and $P_{\nu,k}$ denote the empirical distribution over the local sample $\mathcal{S}_{\nu,k}$. The empirical distribution is defined as the measure assigning mass $1/n$ to each observation. Since the datasets are disjoint, the global empirical measure P_ν is the weighted average of the local measures. For any event E :

$$\begin{aligned} P_\nu(E) &= \frac{1}{n_\nu} \sum_{i \in \mathcal{S}_\nu} \mathbb{1}(y_i \in E) \\ &= \sum_{k=1}^K \frac{n_{\nu,k}}{n_\nu} \left(\frac{1}{n_{\nu,k}} \sum_{i \in \mathcal{S}_{\nu,k}} \mathbb{1}(y_i \in E) \right) \\ &= \sum_{k=1}^K w_{\nu,k} P_{\nu,k}(E), \end{aligned}$$

where $w_{\nu,k} = \frac{n_{\nu,k}}{n_\nu}$ represents the mixture weight of client k .

The global empirical impurity is defined as the function Ψ (mean squared error, Gini, cross entropy etc.) applied to the global distribution P_ν :

$$I(\mathcal{S}_\nu) = \Psi(P_\nu) = \Psi \left(\sum_{k=1}^K w_{\nu,k} P_{\nu,k} \right).$$

We add and subtract the weighted sum of local impurities $\sum_{k=1}^K w_{\nu,k} \Psi(P_{\nu,k})$:

$$\begin{aligned} I(\mathcal{S}_\nu) &= \Psi \left(\sum_{k=1}^K w_{\nu,k} P_{\nu,k} \right) \\ &= \underbrace{\sum_{k=1}^K w_{\nu,k} \Psi(P_{\nu,k})}_{\text{Weighted Local Impurities}} + \underbrace{\left[\Psi \left(\sum_{k=1}^K w_{\nu,k} P_{\nu,k} \right) - \sum_{k=1}^K w_{\nu,k} \Psi(P_{\nu,k}) \right]}_{\text{Heterogeneity Term}} \\ &= \sum_{k=1}^K \frac{n_{\nu,k}}{n_\nu} I(\mathcal{S}_{\nu,k}) + \mathcal{E}(\nu), \end{aligned}$$

which corresponds to (6).

Finally, we show that for strictly concave impurities, $\mathcal{E}(\nu) = 0 \iff \forall(k, k'), \hat{\mathbb{E}}[Y | \mathcal{S}_\nu, H = k] = \hat{\mathbb{E}}[Y | \mathcal{S}_\nu, H = k']$. Let $\mu_{\nu,k} = \hat{\mathbb{E}}[Y | \mathcal{S}_\nu, H = k]$ denote the local empirical mean outcome (regression) or class probability vector (classification).

For regression, the Law of Total Variance identifies $\mathcal{E}(\nu)$ as the variance of these local means: $\mathcal{E}(\nu) = \sum \frac{n_{\nu,k}}{n_\nu} (\mu_{\nu,k} - \mu_\nu)^2$.

For classification, $\mu_{\nu,k}$ is the vector of class probabilities (since $\hat{\mathbb{E}}[Y_{\text{one-hot}}] = \mathbf{p}$), and impurity is defined as $\Psi(\mu_{\nu,k})$ where Ψ is strictly concave (e.g., Gini or Entropy). By Jensen's inequality, the gap $\mathcal{E}(\nu) = \Psi(\sum \frac{n_{\nu,k}}{n_\nu} \mu_{\nu,k}) - \sum \frac{n_{\nu,k}}{n_\nu} \Psi(\mu_{\nu,k})$ is non-negative.

In both cases, due to strict concavity, $\mathcal{E}(\nu) = 0 \iff \mu_{\nu,1} = \dots = \mu_{\nu,K}$, i.e., the mean outcome is identical across sites. \square

A.2. Impurity reduction estimator: homogeneous setting

Proof of Theorem 3.4:

Proof. Recall the definition of the global centralized empirical impurity reduction at node A :

$$\Delta I(j, t; \mathcal{S}_\nu) = I(\mathcal{S}_\nu) - \left[\frac{n_L}{n_\nu} I(\mathcal{S}_L) + \frac{n_R}{n_\nu} I(\mathcal{S}_R) \right].$$

Using the impurity decomposition in Eq. (6), we have:

$$\begin{aligned} I(\mathcal{S}_\nu) &= \sum_{k=1}^K \frac{n_{\nu,k}}{n_\nu} I(\mathcal{S}_{\nu,k}) + \mathcal{E}(A), \\ I(\mathcal{S}_L) &= \sum_{k=1}^K \frac{n_{L,k}}{n_L} I(\mathcal{S}_{L,k}) + \mathcal{E}(L), \\ I(\mathcal{S}_R) &= \sum_{k=1}^K \frac{n_{R,k}}{n_R} I(\mathcal{S}_{R,k}) + \mathcal{E}(R), \end{aligned}$$

which yields:

$$\Delta I(j, t; \mathcal{S}_\nu) = \underbrace{\sum_{k=1}^K \frac{n_{\nu,k}}{n_\nu} \Delta I_k(j, t; \mathcal{S}_{\nu,k})}_{\widehat{\Delta I}_{\text{fed}}} + \underbrace{\left(\mathcal{E}(A) - \frac{n_L}{n_\nu} \mathcal{E}(L) - \frac{n_R}{n_\nu} \mathcal{E}(R) \right)}_{\text{Residual Term } \delta_n}.$$

Thus, the discrepancy is strictly governed by the heterogeneity terms: $|\widehat{\Delta I}_{\text{fed}} - \Delta I| = |\delta_n|$.

We analyze δ_n for the standard impurity measures derived in the previous section.

Variance Impurity (Regression). When impurity is measured as variance, the heterogeneity term \mathcal{E} is explicitly the variance of the local means:

$$\mathcal{E}(\nu) = \sum_{k=1}^K \frac{n_{\nu,k}}{n_\nu} (\bar{y}_{\nu,k} - \bar{y}_\nu)^2.$$

Under Theorem 2.1, each client draws samples from the same population. At node A , the local sample mean at node $\bar{y}_{\nu,k}$ is an unbiased estimator of μ_ν with variance $\mathbb{V}(\bar{y}_{\nu,k}) = \frac{\sigma_\nu^2}{n_{\nu,k}}$. The term $(\bar{y}_{\nu,k} - \bar{y}_\nu)^2$ scales with its variance at $O_p(1/n_{\nu,k})$:

$$\mathcal{E}(\nu) = \sum_{k=1}^K \frac{n_{\nu,k}}{n_\nu} O_p\left(\frac{1}{n_{\nu,k}}\right) = \sum_{k=1}^K O_p\left(\frac{1}{n_\nu}\right) = O_p\left(\frac{K}{n_\nu}\right).$$

Gini and entropy impurities (classification). In classification, the local "mean" corresponds to the vector of class probabilities $\mathbf{p}_{\nu,k}$. For Gini impurity, the heterogeneity term is exactly the weighted squared Euclidean distance between the local and global probability vectors (by the law of total variance):

$$\mathcal{E}_{\text{Gini}}(\nu) = \sum_{k=1}^K \frac{n_{\nu,k}}{n_\nu} \|\mathbf{p}_{\nu,k} - \mathbf{p}_\nu\|^2.$$

For Entropy, the heterogeneity corresponds to the Jensen-Shannon divergence, which acts locally as a quadratic approximation. By a second-order Taylor expansion, it relates to the chi-squared distance:

$$\mathcal{E}_{\text{Entropy}}(A) = \sum_{k=1}^K \frac{n_{\nu,k}}{n_{\nu}} D_{\text{KL}}(\mathbf{p}_{\nu,k} \| \mathbf{p}_{\nu}) \approx \frac{1}{2} \sum_{k=1}^K \frac{n_{\nu,k}}{n_{\nu}} \sum_{c=1}^C \frac{(p_{\nu,k}^{(c)} - p_{\nu}^{(c)})^2}{p_{\nu}^{(c)}}.$$

In both cases, the heterogeneity is driven by the squared norm $\|\mathbf{p}_{\nu,k} - \mathbf{p}_{\nu}\|^2$. Since the empirical class frequencies $\mathbf{p}_{\nu,k}$ deviate from the true population probabilities by a factor of $O_p(1/\sqrt{n_{\nu,k}})$, the squared norm scales as $O_p(1/n_{\nu,k})$.

To conclude, since $\mathcal{E}(L)$ and $\mathcal{E}(R)$ follow the same scaling (with denominators $n_L, n_R < n_{\nu}$), the total residual δ_n is a linear combination of terms that are all $O_p(K/n_{\nu})$. Therefore:

$$\left| \Delta I_n(j, t; \mathcal{S}_{\nu}) - \sum_{k=1}^K \frac{n_{\nu,k}}{n_{\nu}} \Delta I_{n_k}(j, t; \mathcal{S}_{\nu,k}) \right| = O_p\left(\frac{K}{n_{\nu}}\right).$$

□

A.3. Candidate thresholds with quantile sketching

Proof of Theorem 3.1:

Proof. The proof proceeds in two steps: first establishing the error bound for local approximations, and then extending it to the global aggregate.

Step 1: Local Error Bound. Consider a single client k transmitting B exact quantiles q_0, \dots, q_B corresponding to ranks $0, 1/B, \dots, 1$. For any value x falling in the interval $[q_i, q_{i+1}]$, the monotonicity of the CDF implies that the true rank $F_{\nu,k}(x)$ lies within the rank interval $[i/B, (i+1)/B]$. Similarly, the linear interpolant $\hat{F}_{\nu,k}(x)$ constructed by the server is also bounded strictly within $[i/B, (i+1)/B]$. Since both the true function and the approximation are confined to the same interval of height $1/B$, their absolute difference is bounded by that height:

$$\left| \hat{F}_{\nu,k}(x) - F_{\nu,k}(x) \right| \leq \frac{i+1}{B} - \frac{i}{B} = \frac{1}{B}.$$

Step 2: Global Aggregation. We now evaluate the error of the global reconstructed CDF $\tilde{F}_{\nu}(x) = \sum w_k \hat{F}_{\nu,k}(x)$ relative to the true global CDF $F_{\nu}(x) = \sum w_k F_{\nu,k}(x)$, where $w_k = n_{\nu,k}/n_{\nu}$:

$$\begin{aligned} |\tilde{F}_{\nu}(x) - F_{\nu}(x)| &= \left| \sum_{k=1}^K w_k \left(\hat{F}_{\nu,k}(x) - F_{\nu,k}(x) \right) \right| \\ &\leq \sum_{k=1}^K w_k \left| \hat{F}_{\nu,k}(x) - F_{\nu,k}(x) \right| \quad (\text{Triangle Inequality}) \\ &\leq \sum_{k=1}^K w_k \left(\frac{1}{B} \right) \\ &= \frac{1}{B} \sum_{k=1}^K w_k = \frac{1}{B}. \end{aligned}$$

Thus, the global rank error is strictly bounded by $\epsilon = 1/B$, independent of the heterogeneity of the local distributions $F_{\nu,k}$. □

Proof of Theorem 3.2. We consider a fixed node A and a centralized candidate $(j, t_{\text{cent}}) \in \mathcal{T}_{\text{cent}}$. We omit the feature index j in the notation and write F_{ν} and \tilde{F}_{ν} for the pooled empirical CDF and its reconstruction (as in Theorem 3.1). By construction, the federated candidate set for this feature is

$$\mathcal{T}_{\nu}^{(j)} = \left\{ \tilde{F}_{\nu}^{-1}\left(\frac{b}{B}\right) : b = 1, \dots, B-1 \right\}.$$

Hence there exists $t_{\text{fed}} \in \mathcal{T}_\nu^{(j)}$ such that

$$|\tilde{F}_\nu(t_{\text{fed}}) - F_\nu(t_{\text{cent}})| \leq \frac{1}{2B},$$

since the grid points $\{b/B\}$ are spaced by $1/B$. We now bound the induced disagreement in left-child assignments:

$$\frac{1}{n_\nu} \sum_{i \in \mathcal{S}_\nu} \mathbb{1}(\mathbb{1}(x_i \leq t_{\text{cent}}) \neq \mathbb{1}(x_i \leq t_{\text{fed}})) = |F_\nu(t_{\text{fed}}) - F_\nu(t_{\text{cent}})|.$$

By the triangle inequality and Theorem 3.1,

$$|F_\nu(t_{\text{fed}}) - F_\nu(t_{\text{cent}})| \leq |F_\nu(t_{\text{fed}}) - \tilde{F}_\nu(t_{\text{fed}})| + |\tilde{F}_\nu(t_{\text{fed}}) - F_\nu(t_{\text{cent}})| \leq \frac{1}{B} + \frac{1}{2B} = \frac{3}{2B}.$$

□

A.4. Communication reduction methods

A.4.1. TOP- L MAXIMUM GAINS AGGREGATION RECOVERS THE TRUE OPTIMAL FEATURE

Proposition A.1 (Screening consistency under i.i.d. clients). *Consider a node A and let $\Delta\mathcal{I}_\nu(j)$ denote the population (pooled) best gain for feature j . Let j^* be the unique maximizer of $\Delta\mathcal{I}_\nu(\cdot)$ with margin $\gamma := \Delta\mathcal{I}_\nu(j^*) - \max_{j \neq j^*} \Delta\mathcal{I}_\nu(j) > 0$.*

Assume that for client k , the empirical best-gain scores $M_{\nu,k}(j)$ concentrate around their population means with exponential tails (i.e., satisfy a sub-Gaussian tail bound). Then, there exist constants $C_1, C_2 > 0$ such that the probability of the optimal feature j^ falling out of the top- L local ranking decays exponentially with the local sample size $n_{\nu,k}$:*

$$\mathbb{P}(\text{rank}_k(j^*) > L) \leq C_1 d \exp(-C_2 n_{\nu,k} \gamma^2). \quad (7)$$

Proof. The proof relies on decomposing the ranking failure into pairwise estimation errors and applying concentration bounds.

For $L \geq 1$, the event $\{\text{rank}_k(j^*) > L\}$ implies that the optimal feature j^* was empirically outperformed by at least L other features, so $\{\text{rank}_k(j^*) > L\} \subseteq \dots \subseteq \{\text{rank}_k(j^*) > 1\}$, so we can bound the probability of the optimal feature not to be selected by:

$$\mathbb{P}(\text{rank}_k(j^*) > L) \leq \mathbb{P}\left(\bigcup_{j \neq j^*} \{M_{\nu,k}(j) \geq M_{\nu,k}(j^*)\}\right).$$

Now consider a specific suboptimal feature $j \neq j^*$. By definition, the true gain gap is $\Delta\mathcal{I}_\nu(j^*) - \Delta\mathcal{I}_\nu(j) \geq \gamma$. For the empirical scores to reverse this order, i.e. satisfying $M_{\nu,k}(j) \geq M_{\nu,k}(j^*)$, their summed estimation errors for features j and j^* must exceed the margin γ . Specifically, let $\varepsilon_k(\cdot) = M_{\nu,k}(\cdot) - \Delta\mathcal{I}_\nu(\cdot)$ be the estimation noise. The reversal condition implies:

$$\varepsilon_k(j) - \varepsilon_k(j^*) \geq \Delta\mathcal{I}_\nu(j^*) - \Delta\mathcal{I}_\nu(j) \geq \gamma.$$

Finally, we have by the Triangle inequality

$$|\varepsilon_k(j)| + |\varepsilon_k(j^*)| \geq |\varepsilon_k(j) - \varepsilon_k(j^*)| \geq \gamma,$$

so for the difference of errors to exceed γ , at least one of the individual error terms must have a magnitude of at least $\gamma/2$. By the concentration assumption (e.g., Hoeffding's inequality for bounded impurity functions), the probability of such a deviation for any single feature decays exponentially with the sample size:

$$\mathbb{P}\left(|\varepsilon_k(j)| \geq \frac{\gamma}{2}\right) \leq c_1 \exp\left(-c_2 n_{\nu,k} \left(\frac{\gamma}{2}\right)^2\right).$$

Last, applying the union bound over the two error terms for the pair (j, j^*) , and subsequently over all $d - 1$ possible suboptimal features j , we obtain:

$$\mathbb{P}(\text{rank}_k(j^*) > L) \leq \sum_{j \neq j^*}^d 2c_1 \exp\left(-\frac{c_2}{4} n_{\nu,k} \gamma^2\right).$$

Simplifying the constants yields the final bound $C_1 d \exp(-C_2 n_{\nu,k} \gamma^2)$.

□

B. Impurity Decomposition under Covariate Shift

To evaluate a split under heterogeneity efficiently, the heterogeneity term \mathcal{E}_Φ defined in Theorem 3.3 forbids the mere aggregation of local impurity gains. While one could compute $\mathcal{E}_\Phi(\mathcal{S}_\nu)$ explicitly and add it to the weighted local impurities, reconstructing the global impurity directly from sufficient statistics is more efficient. For standard impurity criteria, the global impurity $I(\mathcal{S}_\nu)$ depends only on additive moments of the target variable (e.g., sums of targets or counts of classes). This allows for an efficient one-shot protocol: rather than sharing raw data, clients transmit a compact vector of sufficient statistics $\mathbf{s}_{\nu,k}$.

Because these statistics are linear, the server can reconstruct the global statistics \mathbf{s}_A simply by summing the local vectors: $\mathbf{s}_\nu = \sum_{k=1}^K \mathbf{s}_{\nu,k}$. The server then evaluates the global centralized impurity using $\Psi(\cdot)$:

$$I(\mathcal{S}_\nu) = \Psi(\mathbf{s}_\nu) = \sum_{k=1}^K \frac{n_{\nu,k}}{n_\nu} \Psi(\mathbf{s}_{\nu,k}) + \mathcal{E}_\Phi(A).$$

By computing $\Psi(\mathbf{s}_\nu)$ directly from the aggregated sums, the server implicitly captures the heterogeneity correction $\mathcal{E}_\Phi(A)$, ensuring the exact same split decision as a centralized algorithm.

The impurity reduction for a candidate split (j, t) is finally computed as:

$$\Delta I(j, t; \mathcal{S}_\nu) = \Psi(\mathbf{s}_\nu) - \left[\frac{n_L}{n_\nu} \Psi(\mathbf{s}_L) + \frac{n_R}{n_\nu} \Psi(\mathbf{s}_R) \right].$$

Table 1 details the minimal statistics \mathbf{s} and the corresponding functional Ψ for common loss functions.

Table 1. Definitions of impurity and sufficient statistics. The column $I(\mathcal{S})$ shows the standard centralized definition. The function $\Psi(\mathbf{s})$ computes this same value using only the aggregated statistics \mathbf{s} , allowing for exact federated evaluation.

Objective	Centralized Impurity $I(\mathcal{S}_\nu)$	Federated Impurity $\Psi(\mathbf{s}_\nu)$	Sufficient Statistics $\mathbf{s}_{\nu,k}$
Regression (MSE)	$\frac{1}{n} \sum_{i \in \mathcal{S}_\nu} (y_i - \bar{y})^2$	$\frac{S_\nu^{(YY)}}{n_\nu} - \left(\frac{S_\nu^{(Y)}}{n_\nu} \right)^2$	$\{n_{\nu,k}, S_{\nu,k}^{(Y)}, S_{\nu,k}^{(YY)}\}$
Classification (Gini)	$1 - \sum_{c=1}^C p_c^2$	$1 - \sum_{c=1}^C \left(\frac{n_{A,c}}{n_\nu} \right)^2$	$\{n_{A,k,c}\}_{c=1}^C$
Classification (Entropy)	$-\sum_{c=1}^C p_c \log p_c$	$-\sum_{c=1}^C \frac{n_c}{n} \log \left(\frac{n_c}{n} \right)$	$\{n_{A,k,c}\}_{c=1}^C$

Standard impurity uses sample mean \bar{y} and class probabilities p_c . In sufficient statistics: $S_{\nu,k}^{(Y)} = \sum_{i=1}^{n_{\nu,k}} y_i$, $S_{\nu,k}^{(YY)} = \sum_{i=1}^{n_{\nu,k}} y_i^2$, and $n_{A,k,c} = \sum_{i=1}^{n_{\nu,k}} \mathbb{1}(y_i = c)$.

Note that the heterogeneity term $\mathcal{E}(A)$ takes explicit forms for each impurity measure:

- **Regression (MSE):** $\mathcal{E}(A) = \sum_{k=1}^K \frac{n_{\nu,k}}{n_\nu} (\bar{y}_{\nu,k} - \bar{y}_\nu)^2$
- **Classification (Gini):** $\mathcal{E}(A) = \sum_{k=1}^K \frac{n_{\nu,k}}{n_\nu} \sum_{c=1}^C (p_{A,k,c} - p_{A,c})^2$
- **Classification (Entropy):** $\mathcal{E}(A) = \sum_{k=1}^K \frac{n_{\nu,k}}{n_\nu} \sum_{c=1}^C p_{A,k,c} \log \left(\frac{p_{A,k,c}}{p_{A,c}} \right)$.

However, in practice, the server does not need to compute these terms explicitly, as they are accounted for when evaluating the impurity Ψ on the aggregated sufficient statistics.

C. Exact Midpoint Enumeration

For completeness, we describe how centralized CART split candidates can be reproduced exactly in a federated setting. At a given node A , centralized CART evaluates midpoints between consecutive unique feature values. In principle, this can be achieved federatively by having each client transmit its node-level feature values, which the server merges into a globally sorted list.

Formally, for feature j , let $\{v_{j,(r)}\}_{r=1}^{m_{A,j}}$ denote the sorted unique pooled values at node A . The exact candidate set is

$$\mathcal{T}_v^{\text{all}} = \bigcup_{j=1}^d \left\{ (j, t) : t = \frac{v_{j,(r)} + v_{j,(r+1)}}{2}, 1 \leq r < m_{A,j} \right\}.$$

This procedure exactly matches centralized CART but requires transmitting $O(n_\nu d)$ floating-point values per node and produces up to $d(n_\nu - 1)$ candidates. As such, it is impractical beyond small-scale settings and is not used in our method.

D. Additional Simulations

Definition of the regression function f . To define a complex, nonlinear, tree-like ground-truth $f : \mathbb{R}^d \rightarrow \mathbb{R}$, we distill a tree on an auxiliary dataset sampled over a fixed domain. We draw $N_{\text{aux}} = 10,000$ samples, $x_{\text{aux}} \sim \text{Unif}([-10, 10]^d)$ with $d = 20$, and rescale them to $\tilde{x} \in [0, 1]^d$. We define the auxiliary target as $y_{\text{aux}} = \sum_{j=1}^d \psi_{(j \bmod 3)}(\tilde{x}_j, \tilde{x})$, using three component functions: $\psi_0(z) = \mathbb{1}\{z > 0.5\}$ (step), $\psi_1(z) = \sin(4\pi z)$ (frequency), and $\psi_2(z, \tilde{x}) = \tilde{x}_j \times \tilde{x}_{(j \bmod d)+1}$ (interaction). Finally, we fit a CART regressor of maximum depth 8 on $(x_{\text{aux}}, y_{\text{aux}})$ and define the ground truth $f(\cdot)$ as the resulting outcome function.

D.1. Covariate shift: when local objectives mis-rank global splits

We study two mechanisms by which covariate shift can affect federated split selection. Throughout, `FedForest Quantiles` remains stable because it constructs candidates from a pooled quantile sketch and evaluates them with exact pooled impurities, whereas `FedForest AvgImp` can fail because it optimizes a different objective (the average of local gains).

D.1.1. DISJOINT SUPPORTS

We generate $K = 2$ clients with $n_k = 150$ samples each and features in \mathbb{R}^d (here $d = 5$). Client k draws

$$X_i^{(k)} \sim \mathcal{N}(\mu_k, I_d), \quad \mu_k = ((-1)^k \gamma, 0, \dots, 0),$$

so that increasing $\gamma \geq 0$ creates a growing gap between client supports along the first coordinate, effectively moving the pooled data distribution of (X) from i.i.d. samples Theorem 2.1 when $\gamma = 0$ to a (Gaussian here) bimodal mixture with $\rho_1 = \rho_2 = \frac{1}{2}$. Outcomes follow a step rule on $X^{(1)}$:

$$Y_i = f(X_i) + \varepsilon_i, \quad f(x) = 10 \times \mathbb{1}\{x^{(1)} > 0\}, \quad \varepsilon_i \sim \mathcal{N}(0, \sigma^2),$$

with $\sigma = 1$, so the irreducible MSE is 1. All RF methods are trained with a maximum depth of 8 and 50 trees. Table 2 shows that as γ increases, `FedForest AvgImp` fails to select the pooled-data optimal split ($j = 1, t = 0$), while quantile candidates remain robust and track centralized training.

Table 2. Mean Squared Error (MSE) comparison under Ranking Disagreement (Lower is Better). At higher shift scales ($\delta \geq 2.5$), the local greedy methods (AvgImp) fail to identify the optimal split in the gap between client supports, while global quantile methods remain robust.

Shift (γ)	FedForest AvgImp (X)	FedForest AvgImp (X,H)	FedForest Quantiles (X)	FedForest Quantiles (X,H)	Centralized (X)	Centralized (X,H)
0.0	1.22 ± 0.18	1.22 ± 0.18	1.22 ± 0.22	1.22 ± 0.22	1.22 ± 0.20	1.22 ± 0.21
1.0	1.26 ± 0.22	1.26 ± 0.22	1.20 ± 0.18	1.20 ± 0.18	1.19 ± 0.17	1.19 ± 0.17
2.5	5.86 ± 5.36	5.86 ± 5.36	1.16 ± 0.12	1.16 ± 0.12	1.19 ± 0.17	1.22 ± 0.15
5.0	19.22 ± 3.99	19.22 ± 3.99	1.05 ± 0.04	1.05 ± 0.04	1.06 ± 0.04	1.06 ± 0.04

D.1.2. OVERLAPPING SUPPORTS: FAILURE DRIVEN BY THE HETEROGENEITY TERM

Disjoint supports are not required for AvgImp to fail. Here, both clients have overlapping feature support, but the pooled impurity differs from the weighted average of local impurities due to the heterogeneity term $\mathcal{E}(A)$ in Theorem 3.3. We simulate $K = 2$ clients with

$$X_i^{(k)} \sim \mathcal{N}(\mu_k, \sigma_X^2), \quad \mu_k \in \{-\gamma, +\gamma\}, \quad \sigma_X = 1.5I_d,$$

and a shared conditional model that linear in feature $X^{(1)}$:

$$Y_i = X_i^{(1)} + \varepsilon_i, \quad \varepsilon_i \sim \mathcal{N}(0, \sigma^2).$$

The pooled optimal split is near the pooled population mean (equal to $\mathbb{E}[X] = \frac{1}{2}(-\gamma) + \frac{1}{2}\gamma = 0$ under balanced mixture weights), and every client has data around that point. Nevertheless, as γ grows, $\mathcal{E}(A)$ increases, so maximizing the average local gain can favor thresholds near the client means (around $\pm\gamma$) instead of the pooled optimum. Table 3 confirms this effect: FedForest Quantiles remains close to centralized performance across shifts, while AvgImp degrades as γ increases, despite overlapping supports.

Table 3. Mean Squared Error (MSE) comparison under Ranking Disagreement (Lower is Better). At higher shift scales ($\delta \geq 2.5$), the local greedy methods (AvgImp) fail to identify the optimal split in the gap between client supports, while global quantile methods remain robust.

Shift (γ)	FedForest AvgImp (X)	FedForest AvgImp (X,H)	FedForest Quantiles (X)	FedForest Quantiles (X,H)	Centralized (X)	Centralized (X,H)
0.0	1.22 ± 0.18	1.22 ± 0.18	1.22 ± 0.22	1.22 ± 0.22	1.22 ± 0.20	1.22 ± 0.21
1.0	1.26 ± 0.22	1.26 ± 0.22	1.20 ± 0.18	1.20 ± 0.18	1.19 ± 0.17	1.19 ± 0.17
2.5	5.86 ± 5.36	5.86 ± 5.36	1.16 ± 0.12	1.16 ± 0.12	1.19 ± 0.17	1.22 ± 0.15
5.0	19.22 ± 3.99	19.22 ± 3.99	1.05 ± 0.04	1.05 ± 0.04	1.06 ± 0.04	1.06 ± 0.04

D.2. Covariate and Outcome Shift

We consider the fully heterogeneous regime of Equation (3), where both covariates ($\alpha_k = .5$ and $\gamma_k = 3$) and outcomes ($\delta = 1.5$) vary across clients. Unless stated otherwise, all methods are trained with a common random-forest configuration: $T = 50$ trees, maximum depth 8, minimum leaf size 5, stratified (by client) bootstrap, and feature subsampling \sqrt{d} . We do not center Y locally. When a method supports splitting on the site indicator, we enable Fisher-style optimal grouping of H .

Data are generated with $K = 5$ clients and $n_k = 200$ samples per client in dimension $d = 10$.

Figure 6 shows that our federated FedForest Quantile and AvgImp methods that split on H perform comparatively to their centralized counterpart.

D.3. Heterogeneity diagnostics for adaptive optimization

To balance communication efficiency with predictive performance, we run a lightweight diagnostic step at the root node of the first tree. The goal is to decide whether i.i.d.-specific accelerations (top- L screening, local-gain averaging, and client subsampling) are appropriate, or whether we should default to the fully robust mode (exact split evaluation and quantile candidates).

Covariate shift test. We test for covariate shift by assessing the null hypothesis $H_0 : X \perp\!\!\!\perp H$ using a federated discriminator of clients. Instead of estimating density ratios—either parametrically or via kernel methods with high communication cost—we reuse the impurity-based split selection of federated decision trees by treating the client index H as the target variable. A federated Random Forest is trained to predict H from X using standard CART criteria.

Under H_0 , the feature distributions $P(X|H = k)$ are identical across clients, implying that no split θ can separate samples by site better than random chance. We quantify this using the site impurity gain. For a (j, t) candidate split at a node ν , each client k sends the count of its local samples falling into the left partitions: $n_{L,k} = \sum_{i \in \mathcal{S}_{\nu,k}} \mathbb{1}(x_i^{(j)} \leq t)$, enough to derive $n_{R,k} = n_{\nu,k} - n_{L,k}$. The server then computes the K -class impurity gain for the site variable H :

$$\Delta I_H(j, t; \mathcal{S}_{\nu}) = I_{\text{site}}(\mathcal{S}_{\nu}) - \left(\frac{n_L}{n_{\nu}} I_H(\mathcal{S}_L) + \frac{n_R}{n_{\nu}} I_H(\mathcal{S}_R) \right),$$

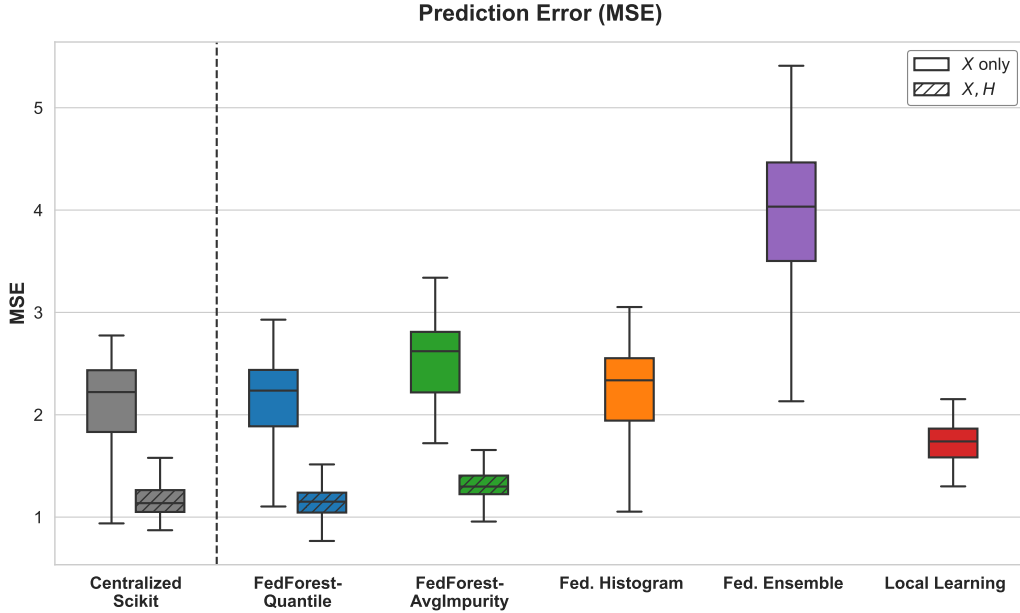


Figure 6. Methods comparison on fully heterogeneous clients (Equation (3)).

where $I_H(\mathcal{S}_L) = 1 - \sum_{k=1}^K \left(\frac{n_{L,k}}{n_L} \right)^2$ (Gini). Note that although each client contains only a single "class" of site labels—i.e., the local impurity is zero—the aggregation of local counts yields the exact global impurity. We thus reject H_0 whenever the maximal root gain or the predictive performance of the site classifier (e.g., one-vs-rest AUC) exceeds a prescribed threshold. This non-parametric technique is federated and further provides interpretable insights on which features are heterogeneously distributed across sites.

Outcome Heterogeneity Test. To detect outcome heterogeneity driven by site effects, one could formally test the null hypothesis that the conditional expectation of the target is invariant across sites. This involves performing $K - 1$ pairwise comparisons (e.g., against a reference site k^*):

$$H_0 : \mathbb{E}[Y | X, H = k] = \mathbb{E}[Y | X, H = k'].$$

While statistical procedures such as permutation tests, Kruskal-Wallis tests on residuals, or cosine similarity tests can be adapted to the federated setting to provide formal significance levels, they typically incur high communication costs and require delicate threshold calibration. Instead, we propose a pragmatic model-based alternative: we compare the validation performance (e.g., accuracy or R^2) of two federated Random Forests—one trained solely on features X , and an augmented model trained on (X, H) . A significant performance gain by the augmented model implies that the site index H contains predictive signal not captured by X , effectively acting as a proxy for rejecting H_0 .